A MAGNETICALLY LEVITATED MOTOR

S. KAZADI, H. SHIN

Abstract. We describe a motor which is built on a floating axle technology. The motor has exactly one point of friction and the weight of the motor can be balanced against the magnetic fields supporting it. We report the design, a model of operation, and the real performance. Limitations in sensor reaction speed and the effect of drag tend to limit speed. Real performance shows good agreement to expected theoretical performance.

1. Introduction

Recent developments in the magnetic bearing system have greatly reduced the effects of these problems. In [1], a self-sensing magnetic bearing is discussed; this bearing uses the same coil which stabilizes the rotor to sense the rotor's position eliminating all position senors. Passive magnetic bearings that not only use no position senors but also no control circuitry have been explored, analyzed, and improved in [2] - [5]. Sucessfull methods to levitate the rotor vertically with no power were achieved with a new magnetic bearing using new arrangements of permanent magnets in [6] - [8]. These bearings use no power for levitation and have a simple control scheme.

In [9], a magnetically levitated axle made using permanent magnets is described. The axle is suspended using a magnetic socket structure which floats vertically above a magnetic ball structure. No sensor system is required and no power is needed for stabilization or levitation.

The development of the epsilon axle makes possible the creation of a new motor whose central axle is the epsilon axle itself. Such a device might have several advantages including very low friction opreation, the ability to statically support a large payload without the concommittant increase in friction or necessity of using high quality bearings. The motor could also be operated in many environments that would generally require specialized materials without them.

This paper describes the design and operation of one such motor. We begin by examining the characteristics of the epsilon axle. We then describe how the epsilon axle can be integrate dinto a motor design and describe its control circuitry. We then explore various opreating characteristics. Finally, we discuss the potential uses and advantages the motor has over the state of the art.

2. $\epsilon-$AXLE

The $\epsilon-$axle is comprised of two main parts. The first part is the magnetic ball and socket. The second part is the axle itself. In [9], Kazadi et. all describe the design and function of the magnetic ball and socket in detail. We will pay more attention to the characteristics of the device. We then examine how the ball and socket may be attached to an axle, illustrating the conditions under which such an axle will be stable.

2.1. Magnetic ball and socket.

The magnetic ball and socket device is comprised of two parts: a magnetic ball designated as the male portion and a magnetic socket designated as the female portion. Both the male and female parts refer to the magnetic fields produced in particular configurations. The combination of these two fields produces forces upon the sources of these magnetic fields that tend to align the sources so that their axes intersect. We designate the source and supporting structures of the magnetic ball as the base. We designated the magnetic socket and its support as the floater. Complete details are given in [9]. Figure 2.1 illustrates the complete ball and socket design.

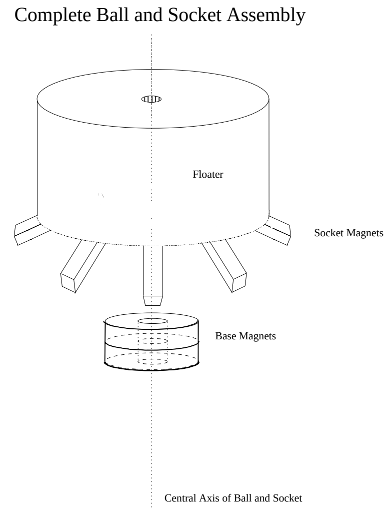

Figure 2.1: The complete ball-and-socket assembly.

The magnetic ball and socket is a self-stabilizing device. The node in the center of the magnetic socket exists because it is at that point that the horizontal components of the repulsion forces between the socket magnets and the base magnet(s) cancel. Deviations from the node result in repulsive forces that tend to move the socket and/or base so as to colocate the node and the magnetic ball. This effect results simply from the geometric structure of the device, requiring no mechanism, external power, or control devices.

If the distance between the floater and the base magnet decreases, the repulsive forces between the two increases. However, as illustrated in Figure 2.4, some configurations have a curious reduction in the repulsion as the distance decreases beyond a minimal distance. Configurations having highly columnated base magnets or magnet assemblies are most strongly affected, particularly those with small diameters with respect to the size of the socket. Using bar magnets to create the socket results in a virtual field reversal in the center of the magnet. This reversed field attracts the base magnet. When the base magnet is close enough to the socket, the effect of the reversed field is to attract the base magnet or magnet assembly.

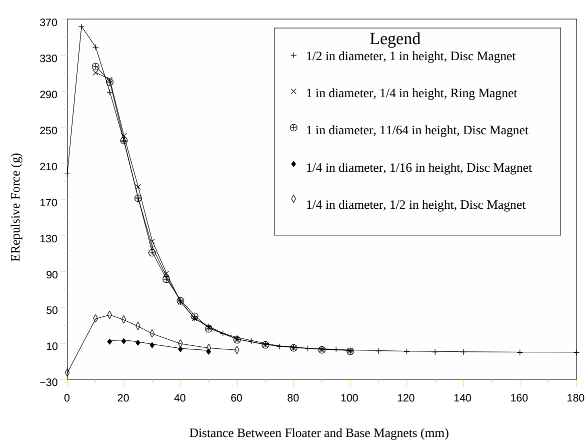

Figure 2.2: This graph shows the force between the magnetic ball and sockets as a function of the distance between them for various base magnets.

Figure 2.2 illustrates the repulsion/attraction force of several configurations. Larger disk magnets whose size is relatively large compared to the socket have a reduction in their attraction, but do not become attracted. This is because thin magnets have a large portion of their magnetic forces aligned with the center field of the socket. Figure 2.5 illustrates the magnetic fields in the magnetic ball and socket system where norths are represented by plus signs and virtual souths represented by minus signs. The maximum repulsive force between the male and female parts is achieved when the base assembly is a ring with a center hole whose size equals that of the reversed field at the center of the socket. When the ball and socket's central axes are aligned, the virtual souths repel each other and do not attract the norths on the magnets while the norths align and add to the repulsive force.

2.2. $\epsilon-$**axle.** An epsilon axle is a magnetic ball and socket device with an attached axle arranged collinearly with the central axis of the socket. The epsilon axle only has one point of contact as it is mechanically supported at one end and magnetically supported at the other. It is illustrated in Figure 2.3.

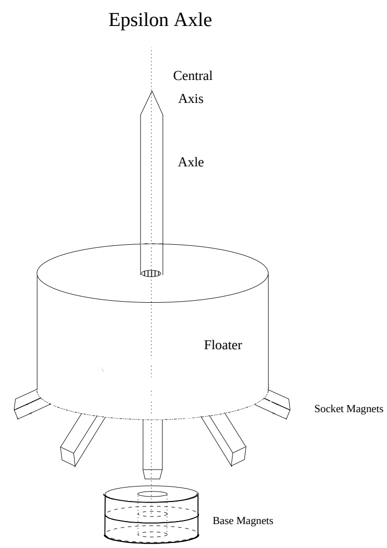

Figure 2.3: A basic axle is connected with the ball and socket device to form the $\epsilon-$axle.

The stability of the axle with respect to vertical perturbations and forces is independent of the length of the axle. Conversely, horizontal perturbations can cause destabilization in two forms. The first is that the socket assembly can come into contact with the base assembly. The second is that the socket can be pushed away from the stationary base assembly, causing a catastrophic collapse of the axle. When a horizontal force is applied on the axle, the whole epsilon axle tilts in a circular arc path where the top of the axle is the center of the circle and the axle is the radius. If the base magnets are in the path, the repulsive force increases as the base and socket assemblies become closer. This tends to keep the parts from coming into contact. If the horizontal force is too great, however, it can overwhelm the repulsion. If the circular arc path does not contain the base magnets, however, a smaller force is required to push the socket enough so that the base magnetic field is outside of the socket, and the repulsive force actually pushes the socket away. In this case, the axle is repelled from the base assembly, and the axle has a catastrophic collapse. The two scenarios are illustrated in Figure 2.7.

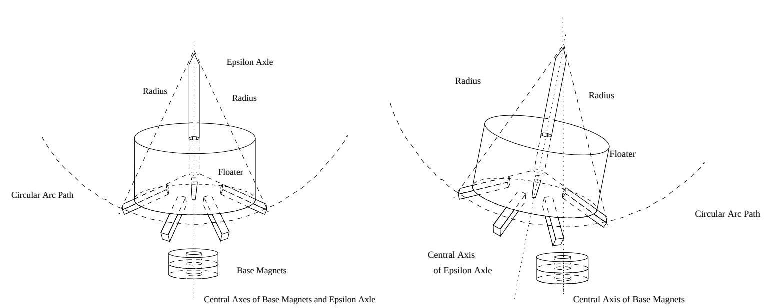

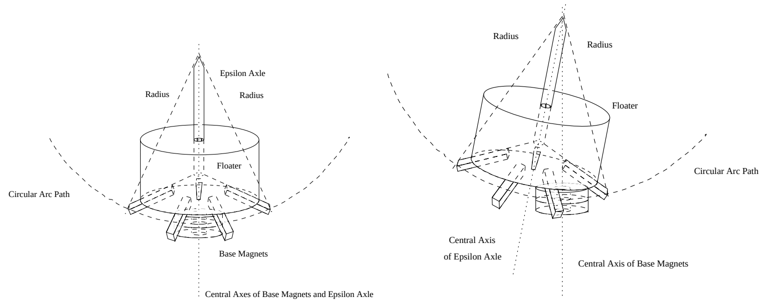

Figure 2.7: The upper two pictures illustrate an unstable mode in which complete destabilization of the $\epsilon-$axle is possible. The bottom two pictures illustrate a stable mode in which complete destablization is not physically possible. Also, the intristic restorative force of the ball and socket is significantly stronger in this stable mode. The $\epsilon-$axles on the left are in the desired vertical position and the pictures on the right demonstrate the results when a horizontal force is applied.

Whether the circular arc path intersects the base magnets or not also depends on the distance between ball and the socket. A shorter distance results in greater stability. If the ball and socket are too far apart from each other, the arc may be above the base magnets instead of containing the magnets in its path. If the base magnets lie in the conical cavity of the socket, then the axle can be any length and the circular arc path will always contain the base magnets.

When the epsilon axle is vertical, the weight of the axle and the load is supported by magnetic fields produced by the ball and socket device. At any other angle, part of the weight is supported by the point of contact on top creating more friction than the vertical arrangement. Therefore, the optimal configuration of the axle is one in which it is aligned with the local gravitational field.

3. The $\epsilon-$motor

It is relatively straightforward to see how the $\epsilon-$axle may be used in a floating motor. In this section we detail the design of an $\epsilon-$motor which utilizes an $\epsilon-$axle as the central rotor. We first consider the mechanical design and then discuss the control circuitry.

3.1. **Mechanical design.** Several criterion are utilized in order to transform an ϵ-axle into a motor.

(1) The motor should be able to withstand a substantial amount of weight whilst also remaining virtually frictionless.
(2) Gears, pulleys, or any other mechanisms requiring physical contact must not be used to convert the motive force as they negate the low friction character of the ϵ-axle.
(3) The payload must be part of or symmetrically attached to the ϵ-axle.

These requirements limit the range of possible designs. We describe one model which satisfies these conditions; we call it the ϵ-motor.

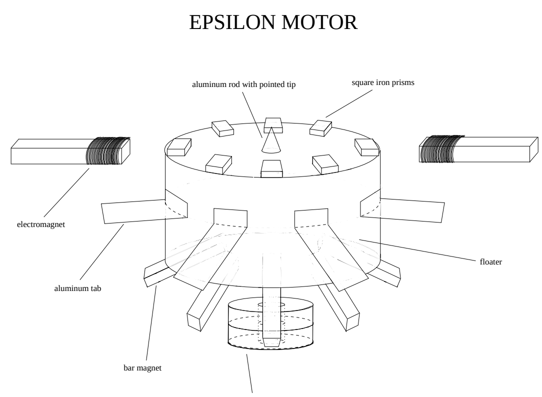

Figure 3.1: This figure illustrates the epsilon motor with all of its components. Its axle's length is minimized.

These requirements can be satisfied by the addition of a small amount of hardware to the basic ϵ-axle. The hardware include eight iron pieces distrubuted equally around the top of the motor, two to six electromagnets on the side surrounding the motor, and eight aluminum tabs distrubted equally around the edge of the motor.

As the motor is stabilized by the ϵ-axle, the stiffness of the central axle is determined by the strength of the repulsion between the ball and socket. In practice, if this repulsion is not strong enough, a strongly attracting electromagnet can pull the floater off center. This can lead to contact between the floater and the electromagnets. To reduce this effect, we utilize pairs of electromagnets which are well balanced, and placed across from one another[1].

The ϵ- motor may be operated in two different modes. In the first mode, the stepper mode, the position of the motor is carefully controlled to within 5°. This is accomplished using six electromagnets to operate the motor, and is generally used for relatively low speed operation. In this mode, magnets are placed around the ring at intervals of sixty (60) degrees. Each pair of magnets on opposite sides of the motor may be operated in sequence. Operating each pair in sequence allows hte motor to make a turn of 5°each time a new pair is energized.

The second mode of operation is the inertial mode. In this mode, the electromagnets are energized when the iron squares are near the electromagnets, and turned off when the iron squares are adjacent the electromagnets. The result is that, with each pulse, the motor increases its rotational speed.

Basic design. We utilize two electromagnets arranged directly across from one another. We utilize aluminum sheets, arranged at forty-five (45) degree intervals. These placements allow the electromagnets to be energized whenever the aluminum plates are in specific locations relative to a stationary sensor. We utilize an infrared sensor arranged so that the aluminum sheets interrupt an IR beam sensed by an IR phototransistor. The control circuitry uses this signal to energize the electromagnets whenever the electromagnets are near the iron squares, and on one side of them. The result is that in each rotation, the electromagnet is energized for a fixed portion of the rotational angle. The situation is illustrated in Figure 3.1.

The Operational Model. It is clear that the operation of the ϵ-motor requires one or more electromagnets. Sets of two balanced electromagnets are required to avoid resonances.

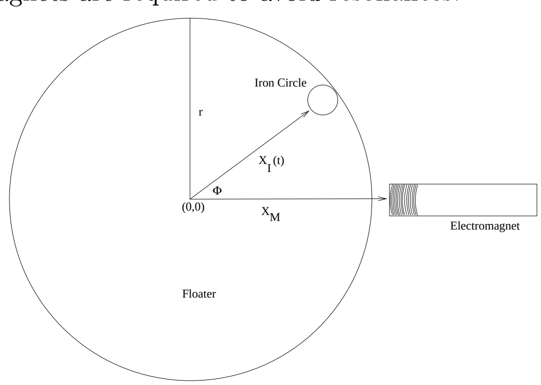

Figure 3.2: Torque on the main rotor.

Consider a single iron piece under the influence of a single magnet and mounted on the main axle of radius r, as illustrated in Figure 3.4. Let $\overrightarrow{x_M}$ be the position of the magnet, $\overrightarrow{x_I(t)}$ is the time dependent position of the iron piece on the main rotor. The the rotational torque is given by the expression

$$\overrightarrow{\tau(t)} = \gamma \frac{\overrightarrow{x_M} \times \widehat{x_I(t)}}{\left|\overrightarrow{x_M} - \overrightarrow{x_I(t)}\right|} \overrightarrow{B\left(\overrightarrow{x_I(t)}\right)} \tag{3.1}$$

where γ is a geometrical factor having to do with the shape of the iron piece, its magnetization, and other properties of the material. In the inertial mode, the magnetic field is only active when the iron piece is closer than α radians to the magnet, where $0 \leq \alpha \leq \frac{\pi}{8}$. Note that $\overrightarrow{x_I(t)} = r(\cos(\phi(t)), \sin(\phi(t)))$ where ϕ is the

[1] Another method is to utilize magnets and ferromagnetic pieces that are very close to the pivot point. This requires a long axle in order to allow space for a payload. This design was not examined in this study.

rotation angle of the central axis. The acceleration due to the magnetic attraction is therefore given by

$$\ddot{\phi_B}(t) = \frac{\gamma}{I} \frac{\widehat{\overrightarrow{x_M} \times \overrightarrow{x_I(t)}}}{\left|\overrightarrow{x_M} - \overrightarrow{x_I(t)}\right|} \overrightarrow{B\left(\overrightarrow{x_I(t)}\right)} \tag{3.2}$$

where I is the moment of inertia of the rotor. Since this acceleration is valid between the limits of $0 \leq \phi \leq \alpha$, the acceleration will only be "on" when the angle is between these limits. Therefore, we have that the total acceleration is given by

$$\ddot{\phi}(t) = \begin{cases} \frac{1}{I}\left(\gamma s(\phi) \frac{\widehat{\overrightarrow{x_M} \times \overrightarrow{x_I(t)}}}{\left|\overrightarrow{x_M} - \overrightarrow{x_I(t)}\right|} \overrightarrow{B\left(\overrightarrow{x_I(t)}\right)} + \mu F_N + \vartheta\left(r\dot{\phi}\right)^3\right) & \left|\dot{\phi}\right| > 0 \\ 0 & \left|\dot{\phi}\right| = 0, \left|\mu F_N\right| > \left|\ddot{\phi_B}(t)\right| \end{cases} \tag{3.3}$$

where μ is the coefficient of sliding friction between the axle and the pivot point, F_N is the normal force of the central axle on the pivot point,

$$s(\phi) = \begin{cases} 1 & 0 \leq \phi mod \frac{\pi}{4} \leq \alpha \\ 0 & otherwise \end{cases}, \tag{3.4}$$

and ϑ is the drag coefficient. Application of this differential equation is illustrated in Figures 3.3 and 3.4.

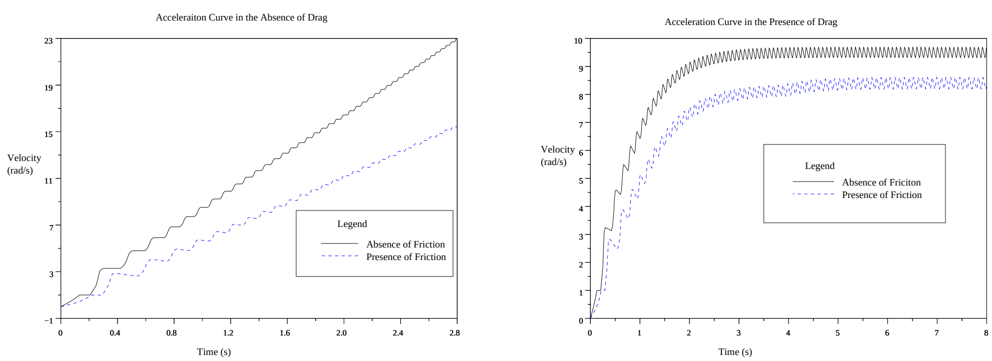

Figure 3.4: The performance of the ϵ-motor in the a) absence amd b) presence of drag.

As depicted in Figure 3.3, the ϵ-motor has an unlimiting speed in the absence of drag, but exhibits a limiting speed in the presence of drag. At this point, the impulse of the magnetic field per cycle equals the total reduction of speed due to the drag and friction, which are continuously active throughout the cycle.

In practice, the two electromagnets are not exactly placed across from one another. Instead, small differences can crop up from improper construction. However, as we can see in Figure 3.4, the ϵ-motor is very robust to skew angles in the absence or presence of drag.

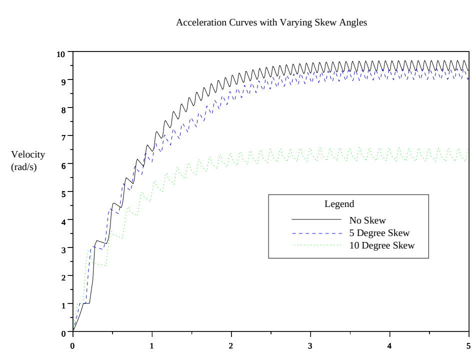

Figure 3.4: The acceleration curve of the ϵ-motor operated in inertial mode using two electromagnets that are not necessarily directly opposite of each other. This graph illustrates the acceleration curve at various skew angles. A skew angle of zero is when the electromagnets are perfectly aligned.

Application of the design to a working model. In application to a real prototype, we utilize a very simple acceleration circuit in order to generate the intertial mode. Figure 3.5 illustrates the ϵ-motor

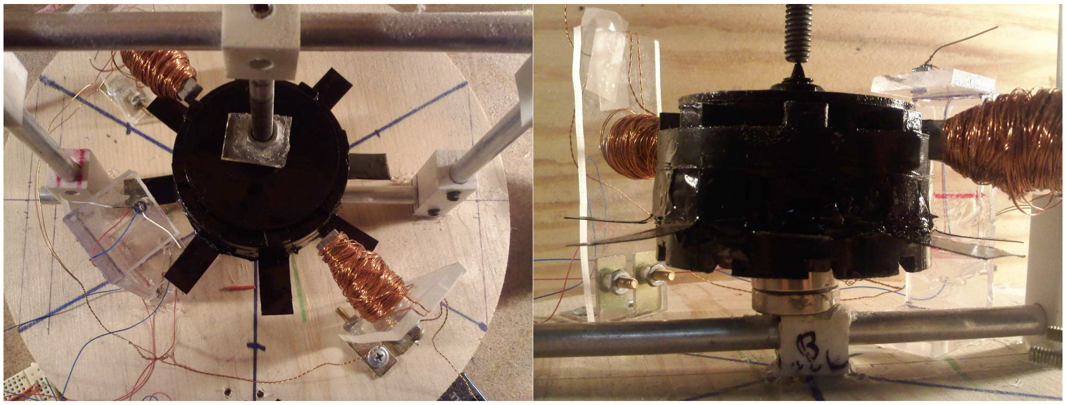

Figure 3.5: A prototype motor, viewed from the side and from below. The view from below elicidates the ϵ-axle.

The circuit utilizes a photodiode switch to control the electromagnets via a power transistor. The circuit energizes the electromagnets when the IR radiation from the photoemitter is interrupted by the aluminum plates on the motor. In practice, the speed of the motor is limited by the switching characteristics of the control circuitry. If the motor is rotating at ω Hz, the aluminum pieces cause a switch on and then off in the space of $\frac{1}{16\omega}$ seconds, as the aluminum pieces subtend less than $\frac{\pi}{8}$ radians. Therefore, if the circuitry has a switching time of τ seconds, the circuit will not come on if the $\frac{1}{16\omega} < \tau$. At that point, the motor has reached its maximum speed.

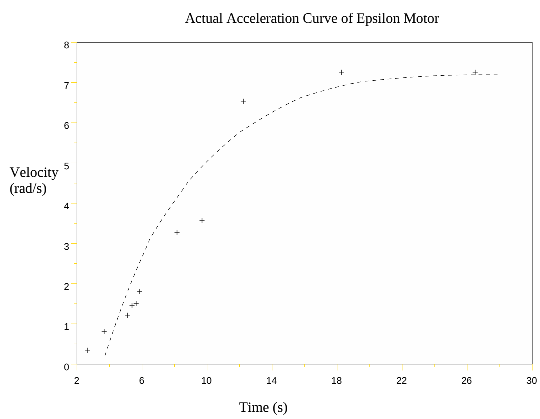

Figure 3.6: Acceleration curve of prototype motor.

As can be seen in Figure 3.9. the results of an acceleration curve of a prototype motor match well with those of a simulated acceleration curve. Our prototype motor exhibits this behavior at 3Hz. At this speed, the photodiode must switch faster than 20.8 ms. Examination of the switching characteristics of the photodiode pair demonstrate this limitation in switching characteristics.

4. Discussion and conclusions

In this paper, we have extended the ϵ-axle by applying it to an actively driven motor device, which we call the ϵ-motor. Such a device has a number of operational advantages owing to the use of the ϵ-axle. The first of these is the capacity to balance the weight of the rotor along with a payload on the rotor. This, in turn, limits the friction and subsequent wear of the rotor, ostensibly increasing its lifetime. Moreover, it reduces the need for high strength components, which may be expensive. Single bearing balls may replace both ball bearing assemblies. This reduces the complexity and cost of the overall motor.

The second advantage derives from the two modes of use of the motor. In one mode, the motor can be used as a high precision stepper motor. The exact rotation per step is dependent on the number of attracting iron pieces on the central axle, and can easily be tuned for any specific application. In the second mode, the same motor can generate very high rotational speeds while using low cost materials in the construction.

Relatively high reliability motors may result from the basic design, allowing very low cost and long lifetime motor designs.

A third advantage is the scalability of the design. Since the design and interaction of magnetic fields is fully scalable, generating very small or very large motors based on these design parameters is extremely straightforward: once a design has been created, scaling it to any size requires no reworking. Rather, the new motor of a different size is identical to the original in every dimension appropriately scaled. The motor function is identical at every scale.

One of the design characteristics of the current design is that actuation is accomplished using electromagnets located at the perimeter of the rotor. As the entire axle is supported by the magnetic field, the stability of the axle, including responsiveness to attractive perturbations and related resonance behaviors, is a function of the forces between the base magnet and the socket. For large rotors with relatively large torques generated by the magnetic attraction, this can lead to significant deviation from equilibrium. Utilizing actuation that is directly on the axle, specifically near the pivot point of the axle, generates significantly less transverse torque. This is expected to generate much lower transverse perturbations. This is the subject of future research.

References

[1] P. Tsao, S. Sanders, and G. Risk. A Self-Sensing Homopolar Magnetic Bearing: Analysis and Experimental Results. In Industry Applications Conference: 34th IAS Annual Meeting, Phoenix, AZ, Oct. 1999.

[2] M. Siebert et. al. A Passive Magnetic Bearing Flywheel. NASA TM No. E-13017. Feb. 2002.

[3] J. Sandtner, J. Bermudez, H. Bleuler. High Speed Passive Magnetic Bearing With Increased Supporting Capabilities. In Seventh International Symp. on Magnetic Bearings, Zurich, Switzerland, Aug. 2000.

[4] T. Takenaga et. al. A Principle And A Design Of A Consequent-Pole Bearingless Motor. In Eighth International Symp. on Magnetic Bearings, Mito, Japan, Aug. 2002.

[5] C. Morrison. Bearingless Switched Reluctance Motor. U.S. Patent 6,727,618 B1, Apr. 2004.

[6] S. C. Mukhopadhyay. Fabrication of a Repulsive-Type Magnteic Bearing Using a Novel Arrangement of Permanent Magnets for Vertical-Rotor Suspension. IEEE Trans. on Mag., vol. 39, no. 5, pp. 3220-3222, Sept. 2003.

[7] T. Ohji et. al. Performance of Repulsive Type Magnetic Bearing System Under Nonuniform Magnetization of Permanent Magnet. IEEE Trans. on Mag., vol. 36, no. 5, pp. 3696-3698, Sept. 2000.

[8] S. C. Mukhopadhyay and C. Goonaratne. Studies of Various Configuration of Permanent Magnetes to Develop Repulsive Type Magnetic Bearing.

[1] S. Kazadi et. al. A Magnetic Ball and Socket, an e-Axle, and a Floating Windmill. 2009.